Journal of Nuclear Materials 386–388 (2009) 971–973

Contents lists available at ScienceDirect

Journal of Nuclear Materials

journal homepage: www.elsevier.com/locate/jnucmat

A numerical study of the size effect in fracture mechanical bending tests with the cohesive zone method

Sabine M. Weygand *, Jarir Aktaa

Forschungszentrum Karslruhe, Institute for Materials Research II, Hermann-von-Helmholtz-Platz 1, 76344 Eggenstein-Leopoldshafen, Germany

A B S T R A C T

A finite element crack growth model is presented which is based on the cohesive zone method and which handles crack initiation and crack growth with a prescribed traction–separation law. In this two parameter approach, the fracture behaviour is determined by the cohesive strength and the separation energy. The model is applied to simulate three-point bending tests of unirradiated reduced-activation ferritic–martensitic steels. The specimen size is varied from nearly standard to miniaturized dimensions to investigate its influence on the crack resistance curve. Additionally, the effect of side grooving on crack initiation and the early stage of crack growth is studied with the presented numerical method.

1. Introduction

Due to the limited irradiation volume provided by IFMIF and other irradiation facilities small specimen testing technologies will be developed particularly for fracture mechanical characterization of irradiated reduced-activation ferritic–martensitic steels (RAFM). Among others miniaturized fracture mechanical three-point bending specimens are considered with the size of Charpy-V subsize specimens (KLST), commonly used in irradiation programs. As plasticity dominates in RAFM steels particularly at temperatures and strain rates within the ranges of application, the requirements for a valid standard test are not met for miniaturized specimens.

Our goal is to establish a method which allows transferring fracture data determined with miniaturized specimens to standard specimens. In this paper, a concept based on the cohesive zone method is presented [1]. This two parameter approach is used in finite element simulations of three-point bending tests where the effect of the specimen size and of side grooving on the crack resistance is studied.

2. Numerical approach (modelling)

2.1. Phenomenological cohesive zone model

Cohesive zones are a suitable method to handle crack initiation and crack propagation with a prescribed traction–separation law [1]. They have already been successfully applied to study the fracture behaviour of ductile [2] and brittle [3] materials. In case of ductile metals like RAFM steels the separation of the cohesive zone originates form the void nucleation and void growth in the process zone around the crack tip. We chose the partly constant traction–separation law (TSL) presented by Scheider and Brocks [4] for ductile behaviour. This law is an idealization of the results of unit cell calculations [2,5]. The main cohesive parameters are the cohesive strength σ_c and the critical separation δ_c or alternatively the separation energy Γ_c. These parameters can be determined by fitting them to experimental curves such as J–R curves and load–displacement curves. A good starting value for Γ_c can be obtained from a fracture test as the value of the J-integral at crack initiation J_{IC} and a reasonable value for the cohesive strength σ_c can be determined from notched tensile tests as the maximum true stress at fracture [3].

For our demonstration example we have chosen a value of 250 N/mm for Γ_c which is the J_{IC} value determined for EUROFER 97 [6] and a value of σ_c of 1500 MPa which corresponds to three times the initial yield stress [5] of a RAFM steel. The additional shape parameters δ_1 und δ_2 shape (for TSL) are taken to be 0.01 and 0.165 mm which results in a critical separation δ_c of 0.173 mm.

2.2. Finite element modelling

As it is common to use Charpy-V subsize specimens (KLST) in irradiation programs, we chose a size of $3 \times 4 \times 27\ \text{mm}^3$ ($B \times W \times L$) for the miniaturized bending specimens. Due to the symmetry it is sufficient to model only one quarter by applying the appropriate symmetry boundary conditions. In accordance with the three-point bending tests performed on EUROFER 97 by Gaganidze et al. [6] the initial crack length of interest is $a_0 = 1.4$ mm leading to an a/W-ratio of 0.35. Cohesive zone elements of the size 0.037 mm × 0.15 mm with eight integration points are placed along the potential crack ligament ($B \times (W - a_0)$) which lies at the middle plane due to pure Mode I occurring during

* Corresponding author.
E-mail address: Sabine.Weygand@imf.fzk.de (S.M. Weygand).

0022-3115/$ - see front matter © 2008 Elsevier B.V. All rights reserved.
doi:10.1016/j.jnucmat.2008.12.264

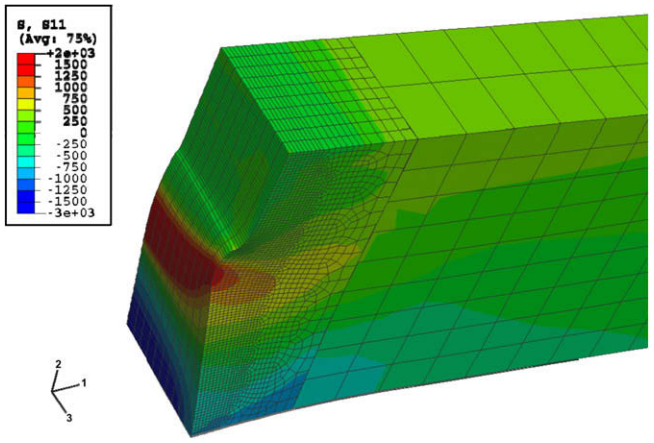

Fig. 1. Finite element model representing one quarter of a miniaturized specimen showing the σ_{11} stress distribution calculated at a load-line displacement of 2 mm. The initial crack length is 1.4 mm and it has extended in average by 0.22 mm.

a bending test. These cohesive zones are implemented in the commercial finite element (FE) code ABAQUS 6.6 as user defined finite elements by use of the user element subroutine UEL developed at GKSS Research Centre Geesthacht [7]. The remaining part of the small specimen is meshed with ordinary 8 noded solid brick elements. The part of the mesh along and around the crack ligament can be seen in Fig. 1. The material behaviour of the continuum finite elements is modelled elasto-plastic with a Young modulus of 210 GPa, an initial yield strength of 500 MPa and strong linear hardening (σ_y = 3000 MPa at ε_{pl} = 0.7) to avoid plastic instabilities. In this first rather qualitative study the selected values of the material properties particularly those of the yield stress and the linear hardening are preliminary and will be later on improved by taking into account the real mechanical behaviour of EUROFER 97 which will allow a reasonable comparison between simulation and experiment in the future. The loading conditions are represented by displacement boundary conditions: (i) support points are restricted in their vertical movement (v = 0) and (ii) points in contact with the loading device are moved in vertical direction with a given cross head speed.

To study the size effect a second mesh has been created for a specimen with three times larger dimensions, namely $9 \times 12 \times 81$ mm^3. To avoid mesh dependency the size of the cohesive zone elements and of the solid finite elements around the crack tip and along the crack ligament remained unchanged.

3. Simulation results

3.1. Influence of the specimen size

The crack growth model presented above was applied to simulate displacement controlled three-point bending tests on miniaturized KLST specimens ($3 \times 4 \times 27$ mm^3) with a distance S between the two specimen supports of 24 mm. As a result Fig. 1 shows the stress distribution of σ_{11} (i.e. normal stress component to the crack plane) computed for a load-line displacement of 2 mm. As due to the higher triaxiality in the inner part the cohesive zones placed there experience higher tractions, consequently the cohesive strength is reached earlier and they separate to a larger extent than the ones near the surface. At the middle line the critical separation δ_c has been already reached in 10 cohesive elements leading to a crack propagation of 0.37 mm while near the surface only three cohesive elements are 'broken' (see Fig. 1). Averaged over the whole thickness the crack length extension Δa is equal to 0.22 mm.

One important result of the FE calculations are load versus load-line displacement curves as they are the basis for the determination of the J-integral with the ASTM standard E 1820 [8]. As in the future we want to compare our numerical results with the experimental crack resistance curves, we apply the same relation to calculate the plastic J-integral J^{pl} as proposed in the ASTM standard for the basic test method:

$$J^{pl} = \frac{2A^{pl}}{B_N(W - a_0)},$$

where A^{pl} corresponds to the area under the load versus plastic load-line displacement curve. B_N stands for the distance between the roots of side-grooved specimens and $B_N = B$ if no side grooves are present.

Additionally to J^{pl} the crack growth Δa is determined for each increment by averaging over the total area of 'broken' cohesive elements divided by B. Note that in contrast to the experimental value this Δa does not include the crack extension due to blunting. In Fig. 2 J^{pl} is plotted versus the corresponding crack extension for the miniaturized specimen.

The same procedure is repeated with the model for the three times larger specimen. Note that only the geometry is changed while material and cohesive parameters remain the same. The resulting crack resistance curve for the larger specimen is also shown in Fig. 2. One can see that it lies below the corresponding curve of the miniaturized which reveals the geometry dependence of $J(\Delta a)$ curves.

3.2. Influence of side grooving

To obtain a straight crack front it is common to side groove the specimens [6]. To analyse their effect with our crack growth model, we modified the mesh of the miniaturized specimen by incorporating V-shaped 0.33 mm deep notches along the ligament. The simulations were repeated for this new geometry. The resulting J–Δa curve is marked in Fig. 2 as dotted line. Right after the initiation it deviates from the curve of the unnotched miniaturized specimen and approaches the curve of the larger specimen.

The lower value for the J-integral can be attributed to the constraint in thickness direction occurring due to the presence of the notch which is confirmed by Fig. 3. There the quarter of the side-grooved specimen is viewed along the horizontal direction looking

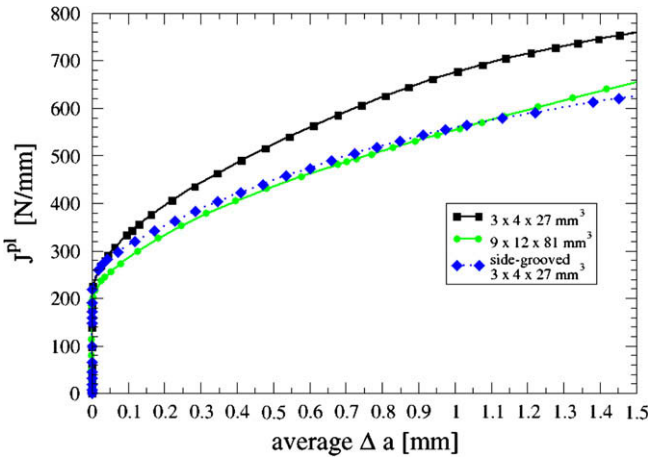

Fig. 2. Crack resistance curves computed numerically for a miniaturized unnotched specimen (marked by the square symbol), for a three times larger unnotched specimen (marked by a circle) and for a miniaturized side-grooved specimen under three-point bending.

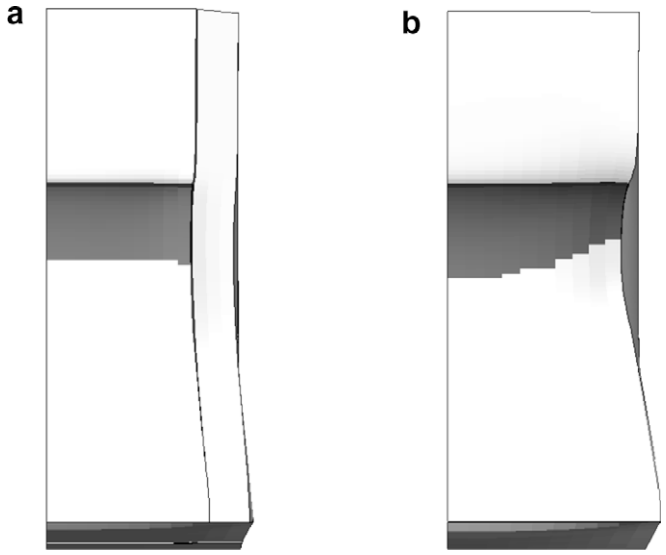

Fig. 3. View on half of the crack ligament showing the crack front for a miniaturized side-grooved specimen at a load-line displacement of 2.2 (a) and on the miniaturized unnotched specimen at a load-line displacement of 2.9 mm (b). In both cases the crack has extended in average by 0.6 mm (on the left side lies the middle line and on the right side there is the free surface).

at the crack ligament revealing the shape of the specimen and the shape of the crack front predicted for a load-line displacement of 2 mm. (see Fig. 3(a)). One can see that only a small contraction occurs in thickness direction in the root of the side groove and that the crack front remains rather straight. For comparison reasons the same view is plotted for the unnotched specimen in Fig. 3(b) for the same average Δa of 0.6 mm. Without a side groove the miniaturized specimen necks stronger resulting in a higher plastic work which is the reason for its higher value of the J-integral.

4. Conclusions and outlook

It is well known that experimentally determined J–Δa curves depend on the geometry of the specimen. In this paper, we could show that our crack growth model based on the cohesive element method can cope with this geometry dependence. With the two cohesive parameters cohesive strength and separation energy it is capable of predicting the different behaviour of small and large three-point bending specimen and of side-grooved specimen. The simulations confirm that side grooving helps in obtaining a straight crack front and that miniaturized side-grooved specimens show a similar behaviour as large specimens. After this rather qualitative study we will fit the cohesive parameters to experimental curves determined with miniaturized specimens, use the same parameters for the prediction of the crack resistance in standard specimens and verify these results.

Acknowledgments

This work, supported by the European Communities under the contract of Association between EURATOM and Forschungszentrum Karlsruhe, was carried out within the framework of the European Fusion Development Agreement. The views and opinions expressed herein do not necessarily reflect those of the European Commission.

References

[1] A. Needleman, Int. J. Fract. 42 (1990) 21.
[2] T. Siegmund, W. Brocks, Eng. Fract. Mech. 67 (2000) 139.
[3] R. Kabir, A. Cornec, W. Brocks, Comput. Mater. Sci. 39 (2007) 75.
[4] I. Scheider, W. Brocks, Eng. Fract. Mech. 70 (2003) 1943.
[5] W. Brocks, SID 1 (4) (2005) 233.
[6] E. Gaganidze, B. Dafferner, J. Aktaa, Forschungszentrum Karlsruhe, FZKA 7252, 2006.
[7] I. Scheider, GKSS Research Centre Geesthacht, GKSS/WMS/06/02, 2006.
[8] ASTM Designation: E 1820-99a, ASTM International, 100 Barr Harbor Drive, West Conshohocken, PA 19428-2959, United States.